Binaries with Mass Ratios Near Unity: The First BVRI Observations, Analysis and Period Studies of TX Canis Minoris and DW Canis Minoris

Ronald G. Samec
Pisgah Astronomical Research Institute, 112 Idlewood Acres, Hartwell, GA 30643; ronaldsamec@gmail.com

Daniel Caton
Jacob Ray
Riley Waddell
Davis Gentry
Dark Sky Observatory, Physics and Astronomy Department, Appalachian State University, 525 Rivers Street, Boone, NC 28608-2106; catondb@appstate.edu

Danny Faulkner
Johnson Observatory, 1414 Bur Oak Court, Hebron, KY 41048; dfaulkner@answersingenesis.org

Received February 25, 2021; revised July 13, 14, 2021; accepted July 14, 2021

Abstract CCD BVRI light curves of TX CMi and DW CMi were taken in 2020 on 20, 21 January, 22, 23 February, and 4 April with the 0.81-m reflector of Appalachian State University by Daniel Caton, Ronald Samec and Danny Faulkner. Six times of minimum light were determined from our present observations of TX CMi. Fifty-five total times of minimum light were included in the 61-year period study. From these we determined that the period for TX CMi is increasing. Eight times of minimum light were determined for DW CMi and thirty-five total times of minimum light were included in the 19.3-year period study. The period is weakly decreasing with a quadratic term of -1.9×10^{-11}. This could be due to mass transfer to M_1 ($q = M2/M_1$) for DW CMi. A Wilson-Devinney (W-D) analysis of TX CMi reveals that the system is a W UMa binary with a mass ratio near unity, q ~1.00. Its Roche Lobe fill-out is ~10%. One spot was needed in the modeling. The temperature difference of the components is only ~90 K, so the stars are nearly twins, with the secondary component the slightly cooler one. The inclination is high, 86.9 ± 0.1°. A W-D analysis reveals that DW CMi is a W-type W UMa binary a mass ratio near unity, q ~1.1. Its Roche Lobe fill-out is ~10%. One weak spot was needed in the modeling. The temperature difference of the components is $T_2 - T_1$ ~260 K, making the binary of W-type.

1. History and observations

1.1. TX CMi

Even though the TX CMi has been known for some 90 years, very little information is known about the binary. We summarize it here. The variability of TX CMi ([GGM 2006] 12715955) was discovered by Hoffmeister (1929). He found it to be a short period variable and little more. It was classified as an EB (β Lyrae) system with a magnitude of V = 13.461 by Gessner (1966). Paschke (1994), using minima from BBSAG bulletins, improved his earlier period (0.3892 d, Paschke 1992) with elements of TX CMi:

$$\text{Min I HJD} = 2436598.611 + 0.3892173\,\text{d} \times \text{E}. \quad (1)$$

Otherwise, a number of times of minima and one low light exist which are noted in the period study.

The system was classified as an EW-type by the All Sky Automated Survey (Shappee *et al.* 2014; Kochanek *et al.* 2017) as ASASSN-V J074019.94+044239.5 (Pojmański 2002). This catalog gives key information: a $V_{mean} = 13.58$, an amplitude of 0.8, and EW designation, J–K = 0.396, B–V = 0.635, E(B–V) = 0.05, and GAIA distance = 794 ± 10 pc. Their ephemeris is:

$$\text{Min I HJD} = 2458023.09677 + 0.3892165\,\text{Ed} \times \text{E}. \quad (2)$$

The ASAS light curve is given in Figure 1.

1.2. DW CMi

DW CMi (GSC2.2 N22123134124) was discovered in 2005 by the SkyDOT team (Polster, Zejda, and Safar 2005) of Copernicus Observatory in Brno, Czech Republic. They gave an R magnitude of 14.3, an EW type, and an ephemeris of:

$$\text{Min I HJD} = 2451965.2876 \pm 0.0009 + 0.30755\,\text{d} \times \text{E}. \quad (3)$$

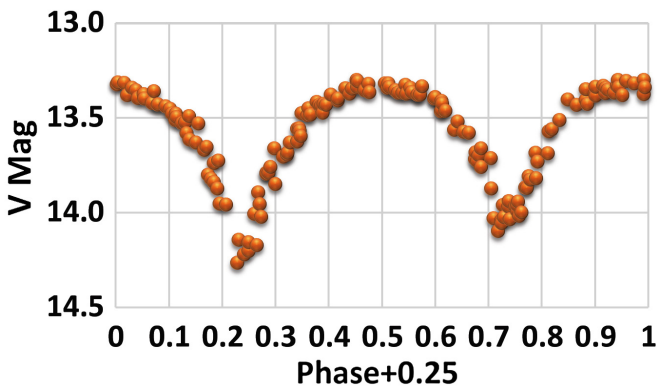

Figure 1. ASAS light curves of TX CMi (Pojmański 2002).

Table 1. Photometric targets.

Star	*Name*	*R.A. (2000)* *h m s*	*Dec. (2000)* ° ′ ″	*V (mag)*	*J–K (mag)*
TX CMi	AN 146.1929 ASAS J074020+0442.7 NSVS 127159566868894	07 40 20.1[1]	+04 42 39.5[1]	14.23	0.396 ± 0.054[1]
DW CMi	GSC2N22123134124 2MASS J07403307+0442200 USNO-A2.0 0900-05269593	07 40 33.0[1]	+04 42 20.1[1]	14.75	0.429 ± 0.062[1]
C (comparison)	GSC 0187 1415 3UC190-079026	07 40 33.0[2]	+04 43 55.90[2]	14.75	0.38
K (check)	GSC 0187 1966	07 40 43.3[1]	+04 42 36.6[1]	10.46	0.256 ± 0.045[1]

[1]*SMBAD.* [2]*UCAC3: The USNO CCD Astrograph Catalog (Zacharias, N., et al. 2010).*

They also gave a position of R.A. (2000) = $07^h\,40^m\,33^s$, Dec. (2000) = +04° 42′ 17″. The only other information published has been times of minimum light (see Table 3, period study table of DW CMi and plots, Figures 10 and 11). The system was observed by the All Sky Automated Survey as ASASSN-V J074032.97+044219.9 (Pojmański 2002). This catalog gives key information: a V_{mean} = 14.65, an amplitude of 0.59, EW designation, J–K = 0.429, B–V = 0.741, E(B–V) = 0.047, and GAIA distance = 904 ± 18 pc. Their ephemeris is:

$$\text{Min I HJD} = 2457322.13402 + 0.3075535\,\text{d} \times \text{E}. \quad (4)$$

The ASAS light curve is given in Figure 2.

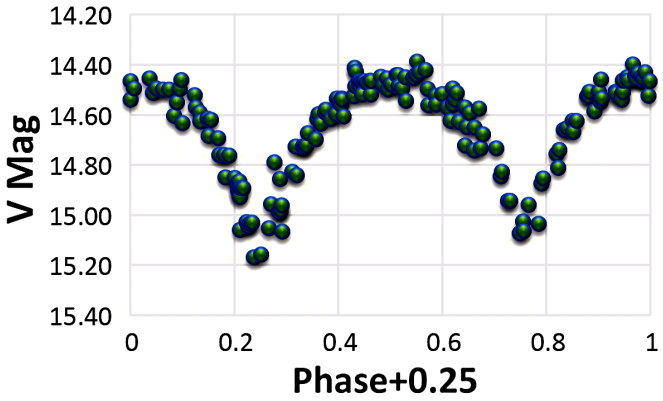

Figure 2. ASAS light curves of DW CMi (Pojmański 2002).

These systems were observed as a part of our professional collaborative studies of interacting binaries at Pisgah Astronomical Research Institute using data taken from DSO observations.

The observations were taken by D. Caton, R. Samec, and D. Faulkner. Reduction and analysis were done by R. Samec.

Our BVR_cI_c light curves were taken at Dark Sky Observatory, on 20, 21, January, 22, 23 February, and 4 April 2020, with a thermoelectrically cooled (–40° C) 2K × 2K Apogee camera and Johnson-Cousins BVR_cI_c filters. Individual observations included 163 in B, 213 in V, 240 in R, and 225 in I. The probable error of a single observation was 9 mmag in B, 11 mmag in V,16 mmag in R, and 18 mmag in I. The nightly C–K values stayed constant throughout the observing run with a precision of about 1.0–1.5% in V. Exposure times varied from 150s in B, 75–100s in V, and 40s in R and I. To produce these images, nightly images were calibrated with 25 bias frames, at least five flat frames in each filter, and ten 300-second dark frames. The early results of this study were presented at the American Astronomical Society meeting #237, 11–15 January (Caton *et al.* 2021; Samec *et al.* 2021).

2. Photometric targets

Table 1 gives basic information on the two variables and the comparison (C) and check (K) stars, including designations, positions, magnitudes, and colors. The finding chart for DW CMi and TX CMi and the comparison and check stars is given in Figure 3.

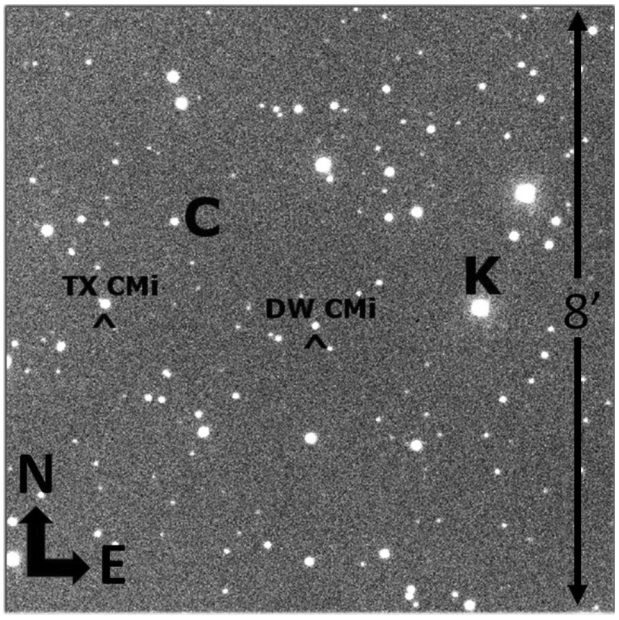

Figure 3. Finding chart (V) for variables TX CMi and DW CMi, comparison (C), and check (K), 4 April 2020.

3. Sample nightly light curves

Two nightly light curves of TX CMi are given as Figures 4 and 5 for 20 and 22 January 2020. Also, nightly light curves of DW CMi are given as Figures 6 and 7 for 20 January and 22 February.

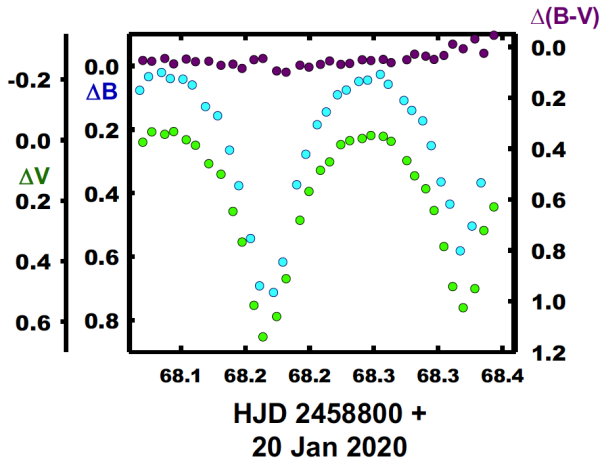

Figure 4. B, V light curves and B–V color curves of TX CMi for 20 January 2020.

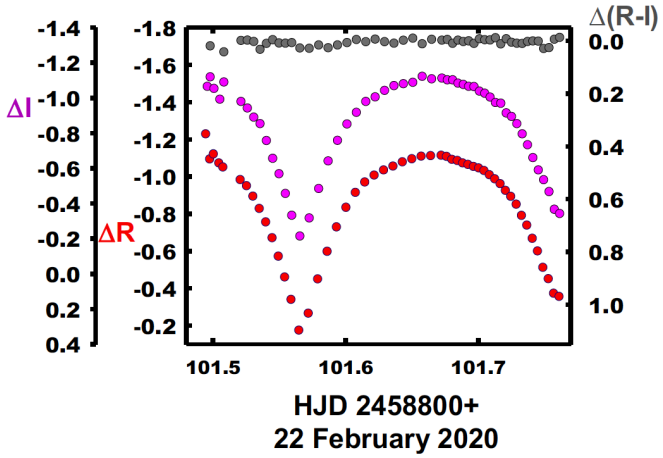

Figure 5. R, I light curves and R–I color curves of TX CMi for 22 February 2020.

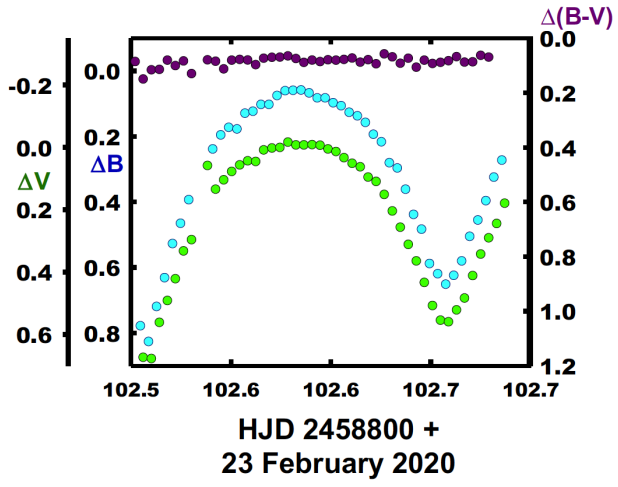

Figure 6. B, V light curves and B–V color curves of DW CMi for 23 February 2020.

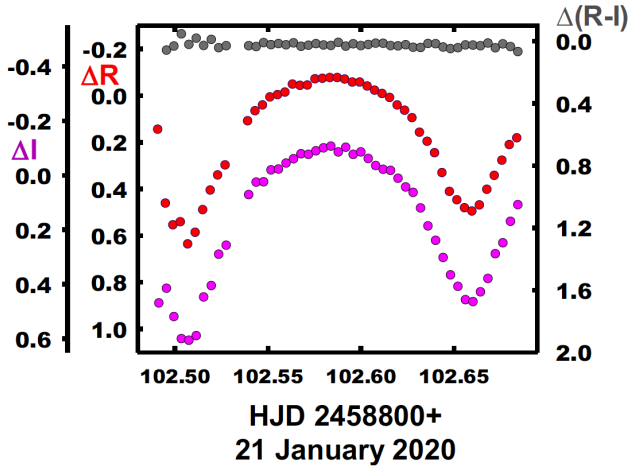

Figure 7. R, I light curves and R–I color curves of DW CMi for 21 January 2020.

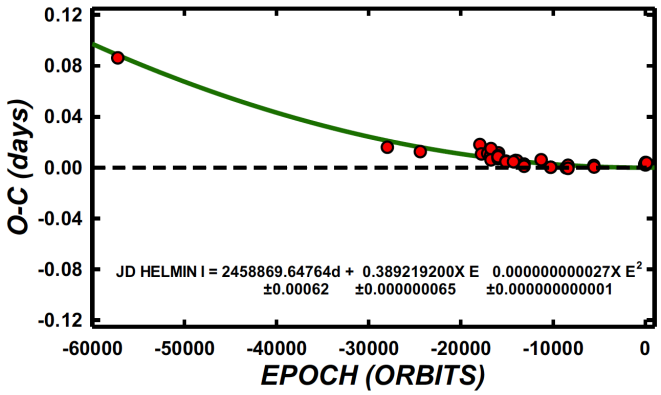

Figure 8. A plot of the quadratic term overlying the linear residuals for TX CMi (showing an increasing period).

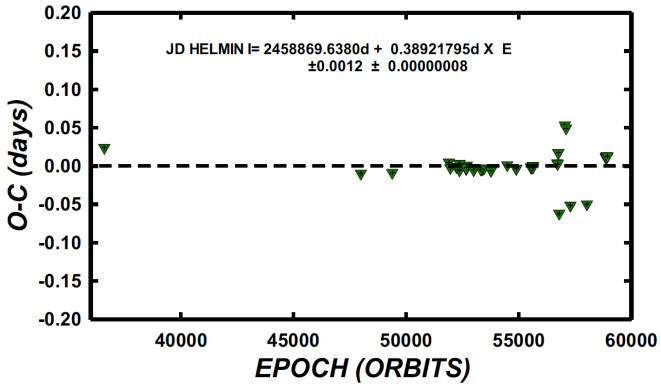

Figure 9. A plot of the linear residuals for TX CMi.

Table 2. Period study TX CMi.

	Epoch	*Cycle*	*Initial Residual*	*Linear Residual*	*Quadratic Residual*	*Wt*	*Reference*
1	36598.6110	–57220.0	0.0378	0.0244	–0.0010	1.0	Paschke (2012)
2	47992.3490	–27946.5	–0.0090	–0.0096	–0.0050	0.1	Paschke (1990)
3	49383.4150	–24372.5	–0.0096	–0.0086	–0.0035	1.0	Paschke (1990)
4	51899.5281	–17908.0	0.0011	0.0049	0.0094	1.0	Brát *et al.* (2007)
5	51968.4125	–17731.0	–0.0061	–0.0023	0.0021	1.0	Brát *et al.* (2007)
6	52230.5521	–17057.5	–0.0051	–0.0009	0.0033	1.0	Brát *et al.* (2007)
7	52692.3610	–15871.0	–0.0038	0.0009	0.0046	1.0	Paschke (2003)
8	53320.9432	–14256.0	–0.0094	–0.0040	–0.0009	1.0	Krajci (2006)
9	53353.8320	–14171.5	–0.0095	–0.0041	–0.0011	1.0	Krajci (2006)
10	53410.2691	–14026.5	–0.0091	–0.0036	–0.0007	1.0	Zejda *et al.* (2006)
11	53410.4645	–14026.0	–0.0083	–0.0028	0.0001	1.0	Zejda *et al.* (2006)
12	53464.3712	–13887.5	–0.0083	–0.0028	0.0001	1.0	Zejda *et al.* (2006)
13	53768.3487	–13106.5	–0.0104	–0.0045	–0.0021	1.0	Hubscher *et al.* (2006)
14	53768.5416	–13106.0	–0.0121	–0.0062	–0.0038	1.0	Hubscher *et al.* (2006)
15	52362.3002	–16719.0	–0.0074	–0.0031	0.0009	1.0	Zejda (2004)
16	52367.3610	–16706.0	–0.0065	–0.0021	0.0019	1.0	Zejda (2004)
17	52367.3614	–16706.0	–0.0061	–0.0017	0.0023	1.0	Zejda (2004)
18	52369.3125	–16701.0	–0.0011	0.0033	0.0073	1.0	Zejda (2004)
19	52369.3036	–16701.0	–0.0100	–0.0056	–0.0016	1.0	Zejda (2004)
20	52668.4196	–15932.5	–0.0083	–0.0036	0.0001	1.0	Zejda (2004)
21	52668.4205	–15932.5	–0.0074	–0.0027	0.0010	1.0	Zejda (2004)
22	52668.4219	–15932.5	–0.0060	–0.0013	0.0024	1.0	Zejda (2004)
23	52668.2266	–15933.0	–0.0067	–0.0020	0.0017	1.0	Zejda (2004)
24	52668.2263	–15933.0	–0.0070	–0.0023	0.0014	1.0	Zejda (2004)
25	52668.2264	–15933.0	–0.0069	–0.0022	0.0015	1.0	Zejda (2004)
26	53000.4215	–15079.5	–0.0097	–0.0047	–0.0013	1.0	Zejda (2004)
27	53000.4210	–15079.5	–0.0102	–0.0052	–0.0018	1.0	Zejda (2004)
28	53318.8024	–14261.5	–0.0095	–0.0041	–0.0010	1.0	Dvorak (2005)
29	54491.7160	–11248.0	–0.0055	0.0012	0.0026	1.0	GCVS (Samus *et al.* 2017)
30	54890.4652	–10223.5	–0.0106	–0.0034	–0.0027	1.0	Samolyk (2010)
31	55553.8889	–8519.0	–0.0097	–0.0017	–0.0023	1.0	Zejda (2004)
32	55554.0835	–8518.5	–0.0097	–0.0017	–0.0023	1.0	Zejda (2004)
33	55554.2781	–8518.0	–0.0097	–0.0017	–0.0023	1.0	Zejda (2004)
34	55554.4727	–8517.5	–0.0097	–0.0017	–0.0023	1.0	Zejda (2004)
35	55554.6673	–8517.0	–0.0097	–0.0017	–0.0023	1.0	Zejda (2004)
36	55554.8619	–8516.5	–0.0097	–0.0017	–0.0023	1.0	Zejda (2004)
37	55555.0565	–8516.0	–0.0097	–0.0017	–0.0023	1.0	Zejda (2004)
38	55555.2511	–8515.5	–0.0097	–0.0017	–0.0023	1.0	Zejda (2004)
39	55555.4457	–8515.0	–0.0097	–0.0017	–0.0023	1.0	Zejda (2004)
40	55555.6404	–8514.5	–0.0097	–0.0017	–0.0023	1.0	Zejda (2004)
41	55555.8350	–8514.0	–0.0097	–0.0017	–0.0023	1.0	Zejda (2004)
42	55556.0296	–8513.5	–0.0097	–0.0017	–0.0023	1.0	Zejda (2004)
43	55556.2242	–8513.0	–0.0097	–0.0017	–0.0023	1.0	Zejda (2004)
44	55621.4197	–8345.5	–0.0082	–0.0002	–0.0010	1.0	Hubscher *et al.* (2012)
45	55625.3126	–8335.5	–0.0075	0.0005	–0.0002	1.0	Hubscher *et al.* (2012)
46	55625.5047	–8335.0	–0.0100	–0.0020	–0.0027	1.0	Hubscher *et al.* (2012)
47	56713.3747	–5540.0	–0.0054	0.0038	0.0006	1.0	Hubscher *et al.* (2015)
48	56726.4123	–5506.5	–0.0067	0.0026	–0.0006	1.0	Hubscher *et al.* (2015)
49	54890.4652	–10223.5	–0.0106	–0.0034	–0.0027	1.0	Samolyk (2010)
50	58868.6769	–2.5	–0.0002	0.0115	0.0023	1.0	Present Observations
51	58869.6501	0.0	0.0000	0.0117	0.0025	1.0	Present Observations
52	58869.8443	0.5	–0.0004	0.0113	0.0021	1.0	Present Observations
53	58901.5674	82.0	0.0014	0.0131	0.0038	1.0	Present Observations
54	58902.5385	84.5	–0.0005	0.0112	0.0019	1.0	Present Observations
55	58943.6028	190.0	0.0012	0.0129	0.0035	1.0	Present Observations

4. Period determination, TX CMi

Six mean times (from BVRI data) of minimum light were calculated from our present observations, three primary and three secondary eclipses:

HJD I = 2458869.65009 ± 0.00030,
2458901.56743 ± 0.00060. 2458943.60276 ± 0.00069

HJD II = 2458868.67688 ± 0.00030, 2458869.84431 ± 0.00060, 2458902.53853 ± 0.000038.

All minima were weighted as 1.0 in the period study except for one time of low light which was weighted 0.1. In total, 55 times of minimum light (References listed in Table 2) were included in this study. This gave us an interval of 61 years.

Table 3. Times of minimum light, DW CMi.

	Epoch	*Cycle*	*Linear Residual*	*Quadratic Residual*	*Wt*	*Reference*
1	51876.5672	–22734.5	0.0054	0.0075	0.5	Polster *et al.* (2006)
2	51899.4704	–22660.0	–0.0043	–0.0022	0.5	Polster *et al.* (2006)
3	51965.2876	–22446.0	–0.0039	–0.0019	0.5	Polster *et al.* (2006)
4	52002.3517	–22325.5	–0.0001	0.0018	0.5	Polster *et al.* (2006)
5	52213.6433	–21638.5	0.0011	0.0027	0.5	Polster *et al.* (2006)
6	53410.3376	–17747.5	–0.0018	–0.0016	1.0	Zejda *et al.* (2006)
7	53410.4915	–17747.0	–0.0016	–0.0015	1.0	Zejda *et al.* (2006)
8	53464.3143	–17572.0	–0.0010	–0.0009	1.0	Zejda *et al.* (2006)
9	53768.3327	–16583.5	–0.0009	–0.0010	1.0	Hubscher and Walter (2007)
10	53768.4862	–16583.0	–0.0012	–0.0013	1.0	Hubscher and Walter (2007)
11	53813.3886	–16437.0	–0.0018	–0.0020	1.0	Hubscher and Walter (2007)
12	54149.3924	–15344.5	–0.0020	–0.0025	1.0	Hubscher and Joachim (2007)
13	55621.3567	–10558.5	0.0033	0.0023	1.0	Hubscher and Lehmann (2015)
14	55621.5096	–10558.0	0.0024	0.0014	1.0	Hubscher and Lehmann (2015)
15	55625.3539	–10545.5	0.0023	0.0012	1.0	Hubscher and Lehmann (2015)
16	55625.5033	–10545.0	–0.0021	–0.0031	1.0	Hubscher and Lehmann (2015)
17	55987.6523	–9367.5	0.0007	–0.0003	1.0	GCVS (Samus *et al.* 2017)
18	56354.4143	–8175.0	0.0032	0.0022	1.0	Hubscher (2015)
19	56713.3313	–7008.0	0.0033	0.0024	1.0	Hubscher and Lehmann (2015)
20	56713.4843	–7007.5	0.0025	0.0016	1.0	Hubscher and Lehmann (2015)
21	56726.4008	–6965.5	0.0017	0.0008	1.0	Hubscher and Lehmann (2015)
22	57039.0275	–5949.0	–0.0014	–0.0022	0.1	ASAS–SN (Shappee *et al.* 2014; Kochanek *et al.* 2017)
23	57100.8501	–5748.0	0.0026	0.0019	0.1	ASAS–SN (Shappee *et al.* 2014; Kochanek *et al.* 2017)
24	57131.7636	–5647.5	0.0068	0.0061	0.1	ASAS–SN (Shappee *et al.* 2014; Kochanek *et al.* 2017)
25	57441.7745	–4639.5	0.0021	0.0016	0.1	ASAS–SN (Shappee *et al.* 2014; Kochanek *et al.* 2017)
26	57757.0166	–3614.5	0.0002	–0.0002	0.1	ASAS–SN (Shappee *et al.* 2014; Kochanek *et al.* 2017)
27	58407.0343	–1501.0	0.0001	0.0003	0.2	ASAS–SN (Shappee *et al.* 2014; Kochanek *et al.* 2017)
28	58868.6736	0.0	–0.0010	–0.0002	1.0	Present Observations
29	58868.8245	0.5	–0.0038	–0.0031	1.0	Present Observations
30	58869.7496	3.5	–0.0014	–0.0007	0.5	Present Observations
31	58901.5827	107.0	–0.0002	0.0005	1.0	Present Observations
32	58901.7360	107.5	–0.0007	0.0001	1.0	Present Observations
33	58902.5052	110.0	–0.0004	0.0003	1.0	Present Observations
34	58902.6583	110.5	–0.0011	–0.0003	1.0	Present Observations
35	58943.5632	243.5	–0.0011	–0.0002	1.0	Present Observations

From these timings, two ephemerides have been calculated, a linear one and a quadratic one:

$$\text{JD Hel Min I} = 24558869.63843 \pm 0.00098\,\text{d} + 0.3892179629 \pm 0.0000000667 \times \text{E}. \quad (5)$$

$$\text{JD Hel Min I} = 2458869.64764 \pm 0.00062\,\text{d} + 0.3892192001 \pm 0.0000000658 \times \text{E} + 0.000000000027 \pm 0.000000000001 \times \text{E2}. \quad (6)$$

Figure 8 shows the quadratic term overlying the linear residuals and Figure 9 gives the linear residuals. Table 2 gives the minima and the residuals of the quadratic and the linear ephemerides.

This TX CMi period study covers an interval of 61 years. It shows an orbital period that is increasing. It might be due to mass transfer to the more massive, component (probably our primary component) making the mass ratio more extreme. Table 2 give the residuals of the linear and quadratic ephemerides. The initial ephemeris was HJD Min I = 2458869.650088 + 0.3892184012 × E.

5. Period determination, DW CMi

Eight mean times (from BVRI data) of minimum light were calculated from our present observations, three primary and five secondary eclipses:

HJD I = 2458868.67357 ± 0.00090, 2458901.5827 ± 0.0004, 2458902.5052 ± 0.0019

HJD II = 2458868.82446 ± 0.00030, 2458869.74956 ± 0.00017, 2458901.7360 ± 0.0008, 2458902.65829 ± 0.00022, 2458943.56315 ± 0.00022

All minima were weighted as 1.0 in the period study except for the ASAS-SN times of low light which was weighted 0.1. In total, 35 times of minimum light (References listed in Table 3) were included in this study. This gave us an interval of 19.3 years.

From these timings, two ephemerides have been calculated, a linear one and a quadratic one:

$$\text{JD Hel Min I} = 2458868.67452 \pm 0.00041\,\text{d} + 0.307555157 \pm 0.000000034 \times \text{E}. \quad (7)$$

Table 4. Light curve characteristics, TX CMi.

Filter	*Phase Min I*	*Mag ± σ*	*Phase Max I*	*Mag ± σ*
	0.00		0.25	
B	–0.093	0.021	–1.091	0.002
V	–0.167	0.024	–1.100	0.005
R	–0.173	0.003	–1.105	0.008
I	–0.274	0.061	–1.090	0.024
Filter	*Phase Min II*	*Mag ± σ*	*Phase Max II*	*Mag ± σ*
	0.5		0.75	
B	–0.316	0.012	–1.155	0.017
V	–0.326	0.007	–1.158	0.005
R	–0.361	0.034	–1.160	0.006
I	–0.341	0.001	–1.146	0.027

Filter	*Min I – Max I*	*± σ ± σ*	*Max I – Max II*	*± σ ± σ*	*Min I – Min II*	*± σ ± σ*
B	0.998	0.023	0.064	0.019	0.223	0.033
V	0.933	0.029	0.058	0.010	0.159	0.031
R	0.932	0.011	0.055	0.014	0.188	0.037
I	0.816	0.085	0.056	0.051	0.067	0.062

Filter	*Min II – Max I*	*± σ ± σ*	*Min I – Max II*	*± σ ± σ*	*Min II – Max I*	*± σ ± σ*
B	0.775	0.013	1.062	0.038	0.775	0.013
V	0.774	0.012	0.991	0.029	0.774	0.012
R	0.744	0.042	0.987	0.010	0.744	0.042
I	0.749	0.025	0.872	0.088	0.749	0.025

Table 5. Light curve characteristics, DW CMi.

Filter	*Phase Min I*	*Mag ± σ*	*Phase Max I*	*Mag ± σ*
	0.00			0.25
B	0.787	0.037	0.058	0.008
V	0.665	0.037	–0.013	0.009
R	0.585	0.006	–0.067	0.011
I	0.518	0.008	–0.099	0.022
Filter	*Phase Min II*	*Mag ± σ*	*Phase Max II*	*Mag ± σ*
	0.5			0.75
B	0.622	0.022	0.026	0.008
V	0.553	0.008	–0.032	0.022
R	0.487	0.009	–0.087	0.010
I	0.432	0.040	–0.116	0.036

Filter	*Min I – Max I*	*± σ ± σ*	*Max I – Max II*	*± σ ± σ*	*Min I – Min II*	*± σ ± σ*
B	0.729	0.045	0.032	0.016	0.165	0.059
V	0.678	0.046	0.019	0.030	0.112	0.045
R	0.652	0.016	0.020	0.021	0.098	0.014
I	0.617	0.030	0.017	0.058	0.086	0.047

Filter	*Min II – Max I*	*± σ ± σ*	*Min I – Max II*	*± σ ± σ*	*Min II – Max II*	*± σ ± σ*
B	0.564	0.030	0.761	0.045	0.596	0.03
V	0.566	0.017	0.697	0.059	0.585	0.03
R	0.554	0.019	0.672	0.015	0.574	0.018
I	0.531	0.062	0.634	0.043	0.548	0.076

JD Hel Min I = 2458868.67380 ± 0.00042 d + 0.30755479 ± 0.00000009 × E–0.000000000019 ± 0.000000000005 × E2. (8)

The residuals of the quadratic and linear ephemerides are given in Table 3.

The phased BVRI light curves and B–V and R–I color curves of TX CMi and DW CMi are given in Figures 12, 13, 14, and 15.

6. Light curve characteristics

6.1.TX CMi

The curves are of fair accuracy, averaging better than 2% photometric precision. The amplitude of the light curves varies from 0.87–1.1 mags from B to I filters. The O'Connell effect, an indicator of spot activity, averages 0.06 mag, which indicates the existence of spots. The differences in minima are appreciable, from 0.07 to 0.22 mag, I to B, respectively, indicating a fair difference in component temperatures. The secondary amplitude averages 0.75 mag, large for a contact binary. The light curve characteristics of TX CMi are given in Table 4.

6.2. DW CMi

Again, the DW CMi curves are of good accuracy, averaging about 2% photometric precision. The amplitude of the light curve varies from 0.76–0.63 mag from B to I filters. The O'Connell effect averages 0.03 mag in B and 0.02 mag in VRI, which indicates the existence of weak spots. The differences in minima are appreciable, from, 0.09 to 0.17 mag, I to B, respectively, indicating a small difference in component temperatures. The secondary amplitude is 0.60, 0.585, 0.58, 0.55 mag, B to I, which is fairly large for a contact binary. The light curve characteristics of DW CMi are given in Table 5.

7. Temperatures

The 2MASS J–K = 0.396 ± 0.054 for TX CMi and B–V = 0.635, E(B–V) ~ 0.05. These correspond to ~G5V ± 2, which yields a temperature of 5750 ± 200 K. Fast rotating binary stars of this type are noted for being magnetic in nature, so the binary is of solar-type with a convective atmosphere.

The J–K for DW CMi = 0.429 ± 0.062 and B–V = 0.741, E(B–V) = 0.047. These correspond to ~G8V±2, which yields a temperature of 5500±200 K.

8. Light curve solutions, TX CMi

The B,V,R_c and I_c curves of TX CMi were pre-modeled with Binary Maker 3.0 (Bradstreet and Steelman 2002). Fits were determined in all filter bands and the results were tabulated. The solutions were that of a shallow contact eclipsing binary. The parameters were then averaged (q or mass ratio = 0.9, fill-out = 0.05, i or inclination = 88, T_2 = 5562.5, and one cool spot with t-fact ($T_{spo}t/T_{photosphere}$) 0.87) and input into a 4-color simultaneous light curve calculation

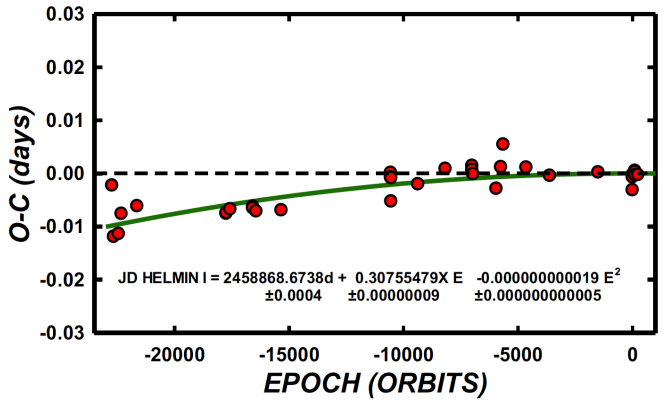

Figure 10. A plot of the quadratic term overlying the linear residuals for DW CMi (showing weakly decreasing period).

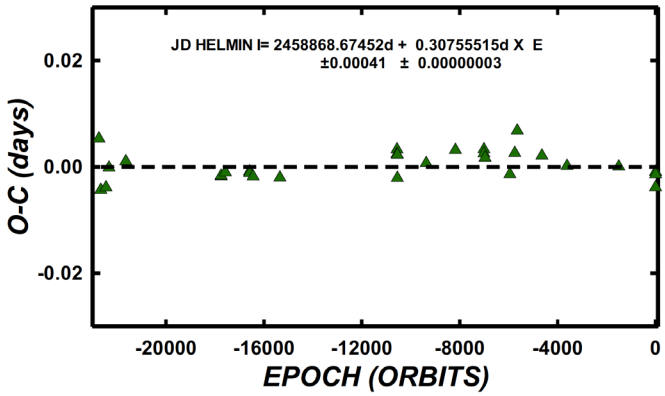

Figure 11. A plot of linear residuals of DW CMi.

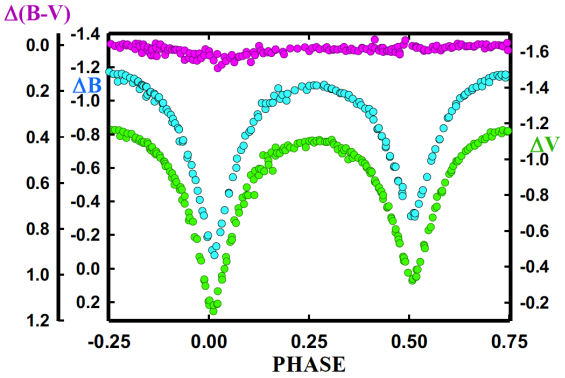

Figure 12. B, V light curves and B–V color curves of TX CMi.

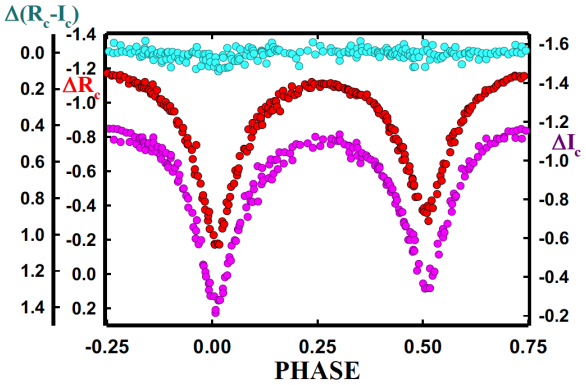

Figure 13. R, I light curves and R–I color curves of TX CMi.

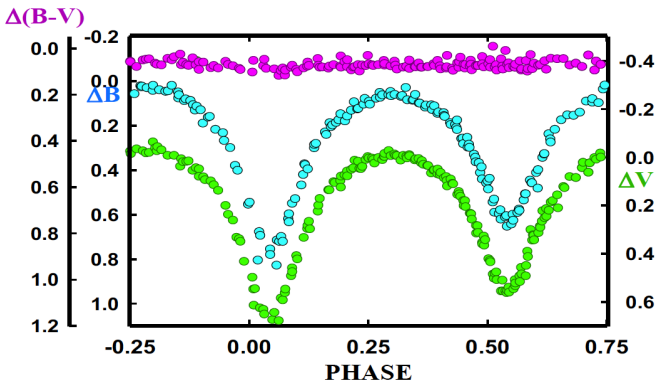

Figure 14. B, V light curves and B–V color curves of DW CMi.

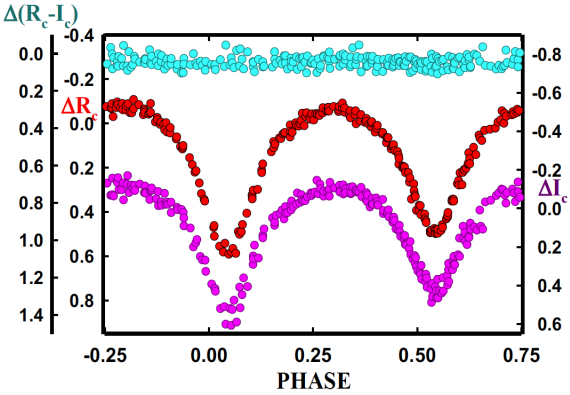

Figure 15. R, I light curves and R–I color curves of DW CMi.

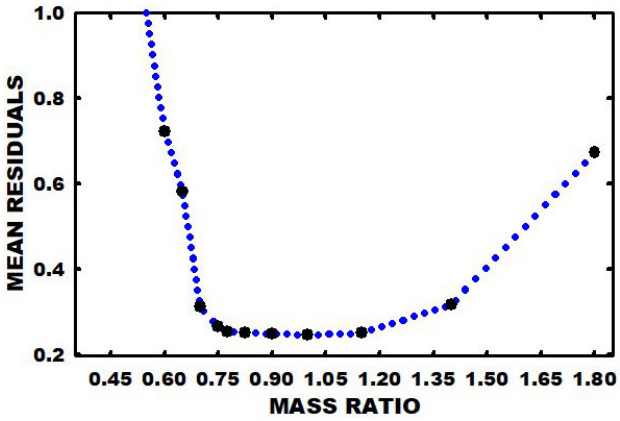

Figure 16. q-search for TX CMi, solutions with fixed mass ratio vs. solution residual.

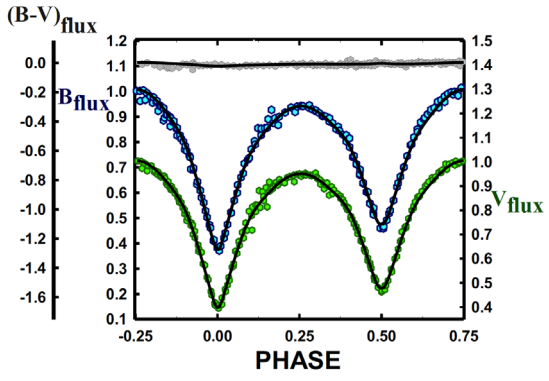

Figure 17. TX CMi B,V normalized flux curves and B–V color curves overlain by B,V solutions.

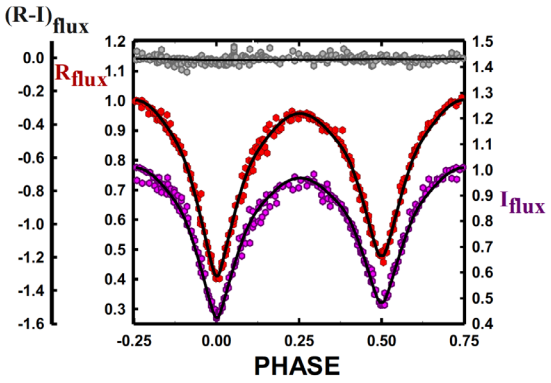

Figure 18.TX CMi R_c,I_c normalized flux curves and R_c–I_c color curves overlain by R_c, I_c solutions.

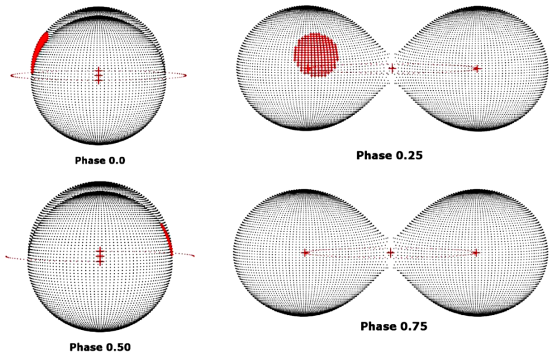

Figure 19. Geometrical representations of TX CMi at quadratures.

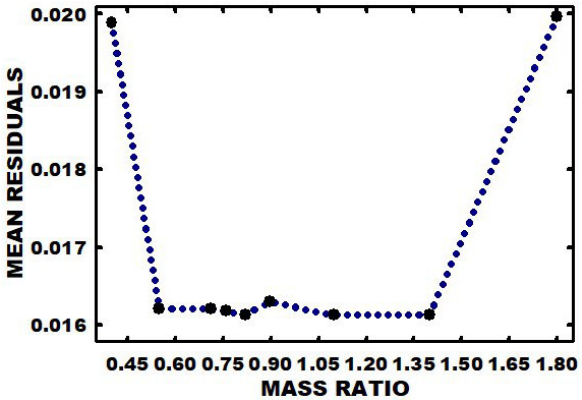

Figure 20. DW CMi, q-search with fixed mass ratio vs. the solution residual.

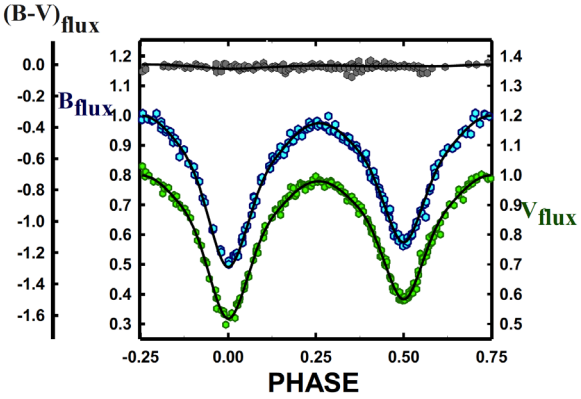

Figure 21. DW CMi B, V normalized flux curves and B–V color curves overlain with B, V solutions.

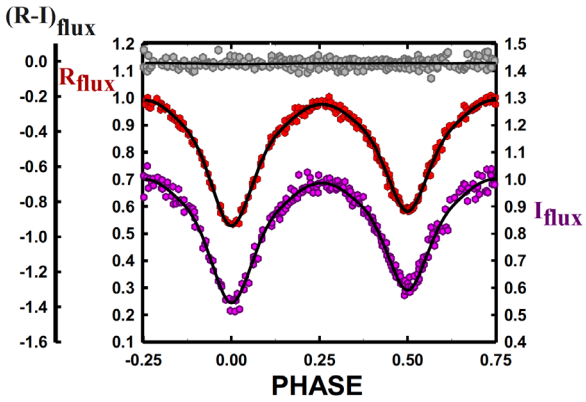

Figure 22. DW CMi R, I normalized flux curves and R–I color curves overlain with R, I solutions.

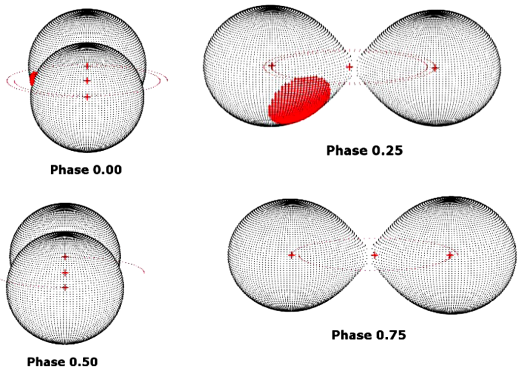

Figure 23. DW CMi geometrical representations at quadratures.

using the Wilson-Devinney Program (W-D; Wilson and Devinney 1971; Wilson 1990, 1994; van Hamme and Wilson 1998). The initial computation was in Mode 3 and converged to a solution (q ~ 0.7). Because there was no total eclipse, a q-search was instigated. In a q-search, a solution is produced for fixed mass ratios. The sum of square residuals is listed for each. The smallest residual is considered to belong to the best estimate of the mass ratio. The minima was fairly broad, with similar residuals between q ~ 0.8 and q ~ 1.15 and the very best goodness of fit residual was at a minima of q = 1.0. The q-search is shown in Figure 16. Convective parameters, g = 0.32, A = 0.5 were used. The q = 1.0 solution is given in Table 6. Figures 17 and 18 show the BVR_cI_c flux overlaid by the light curve solutions. Geometric representations of the surface of the binary at quadratures are given in Figure 19. Table 7 gives the system dimensions and Table 8 gives absolute parameters.

9. Light curve solutions, DW CMi

As with TX CMi, the B,V,R_c and I_c curves were pre-modeled with Binary Maker 3.0. Fits were determined in all filter bands and the results were tabulated. The results were, again, that of a shallow contact eclipsing binary. The averaged parameters were q = 0.7, fill-out = 0.05, i = 78.5°, T_2 = 5300 K, and one cool spot with t-fact = 0.91 and was followed by analysis by the W-D program. The initial computation was in Mode 3 and converged to a solution

Table 6. B,V,R_c,I_c Wilson-Devinney program solution parameters, TX CMi.

Parameter	*Value*
λ_B, λ_V, λ_R, λ_I (nm)	440, 550, 640, 790
g_1, g_2	0.32
A_1, A_2	0.5
Inclination (°)	86.91 ± 0.13°
T_1, T_2 (K)	5750, 5559 ± 1
Ω	3.6953 ± 0.0028
$q(m_2/m_1)$	1.002 ± 0.002
Fill-outs: $F_1 = F_2$ (%)	0.10 ± 0.01
$L_1/(L_1+L_2+L_3)_I$	0.5277 ± 0.0009
$L_1/(L_1+L_2+L_3)_R$	0.5321 ± 0.0011
$L_1/(L_1+L_2+L_3)_V$	0.5381 ± 0.0007
$L_1/(L_1+L_2+L_3)_B$	0.5514 ± 0.0007
JD_o (days)	2458868.8713 ± 0.0001
Period (days)	0.38921992 ± 0.0000009
r_1/a, r_2/a (pole)	0.363 ± 0.002, 0.363 ± 0.0002
r_1/a, r_2/a (side)	0.382 ± 0.002, 0.382 ± 0.002
r_1/a, r_2/a (back)	0.417 ± 0.003, 0.417 ± 0.003
Spots, Star 1	
Colatitude (°)	74.6 ± 2.4°
Longitude (°)	282.3 ± 0.7°
Radius (°)	20.2 ± 0.4°
T-factor	0.781 ± 0.009

Table 7. TX CMi system dimensions.

R_1, R_2 (pole, $R_\odot$)[1]	1.005 ± 0.0006	1.005 ± 0.0006
R_1, R_2 (side, $R_\odot$)[1]	1.058 ± 0.0006	1.058 ± 0.0006
R_1, R_2 (back, $R_\odot$)[1]	1.154 ± 0.0007	1.154 ± 0.0007

[1]*Using a = 2.76778 $R_\odot$.*

Table 8. Estimated TX CMi absolute parameters.[1]

Parameter	*Star 1*	*Star 2*
Mean radius ($R_\odot$)	1.071	1.071
Mean density	1.078	1.078
Mass ($M_\odot$)	0.94	0.94
Log g	4.42	4.42

[1]*Density units are gm/cm³. a = semi-major axis.*

Table 9. DW CMi Solution synthetic light curve parameters.

Parameter	*Value*
λ_B, λ_V, λ_R, λ_I (nm)	440, 550, 640, 790
g_1, g_2	0.32
A_1, A_2	0.5
Inclination (°)	78.36 ± 0.08
T_1, T_2 (K)	5500, 5244.4 ± 1.8
Ω	3.8864 ± 0.0034
$q(m_2/m_1)$	1.100 ± 0.002
Fill-outs: $F_1 = F_2$ (%)	4.5
$L_1/(L_1+L_2+L_3)_I$	0.5202 ± 0.0006
L1/(L1+L2)R	0.5270 ± 0.0057
$L_1/(L_1+L_2+L_3)_V$	0.5369 ± 0.0016
$L_1/(L_1+L_2+L_3)_B$	0.5553 ± 0.0011
JD_o (days)	2458868.67318 ± 0.00011
Period (days)	0.3075569 ± 0.000001
r_1/a, r_2/a (pole)	0.351 ± 0.002,0.367 ± 0.002
r_1/a, r_2/a (side)	0.369 ± 0.003,0.386 ± 0.003
r_1/a, r_2/a (back)	0.402 ± 0.005,0.418 ± 0.004
Spots, Star 1	
Colatitude (°)	119.8 ± 1.5
Longitude (°)	306.6 ± 4.3
Spot radius (°)	30.85 ± 1.01
T-factor	0.939 ± 0.003

Table 10. DW CMi system dimensions.

R_1, R_2 (pole, $R_\odot$)	0.844 ± 0.006	0.882 ± 0.006
R_1, R_2 (side, $R_\odot$)	0.887 ± 0.007	0.929 ± 0.007
R_1, R_2 (back, $R_\odot$)	0.965 ± 0.011	1.010 ± 0.010

Table 11. DW CMi estimated absolute parameters.[1]

Parameter	*Star 1*	*Star 2*
Mean Radius ($R_\odot$)	0.899	0.939
Mean Density	1.755	1.819
Mass ($M_\odot$)	0.906	0.997
Log g	4.48	3.49

[1]*a = semi-major axis. Density units are gm/cm³.*

(q ~ 0.7). As with TX CMi, a q-search was instigated. The minima of the curve was very broad, with similar residuals between q ~ 0.4 and q ~ 1.4 and the very best goodness of fit residual was at a minima of q = 1.1. The q-search is shown in Figure 20. Again, convective parameters, g = 0.32, A = 0.5 were used. The q = 1.1 solution follows in Table 9. The system dimensions are given in Table 10 and absolute parameters in Table 11. The B, V, R, I normalized flux curves and B–V and R, I color curves overlain with the solutions are given in Figures 21 and 22. The geometric system representations at quadrature's are given in Figure 23.

10. Discussion

TX CMi is shallow contact W UMa binary. As stated earlier, the q-search minimized at 1.0. The system's fill-out is 10%, and a component temperature difference is a ~ 190 K, so the stars are very similar in spectral type. One spot was needed in the solution, a Northern, 15° latitude, 20° radius spot with a t-fact of 0.78. The inclination of ~ 86.9 degrees did not result in a time of constant light in due to the similar sizes of the components. Its photometric spectral type indicates a surface temperature of ~ 5750 K for the primary component, making it a solar-type binary. Such a main sequence star would have a mass of ~ 0.98 $M_\odot$ and the secondary (from the mass ratio) would have a mass of ~ 0.965 $M_\odot$, making the stars nearly twins.

DW CMi is a shallow contact (4.5%) W-type W UMa binary (if the q = 1.1 (0.002) solution is correct). The component temperature difference was about 255 K, which is reasonable for the shallow contact. The spot was a Southern cool spot with a t-fact of 0.938, –30° latitude, 31° radius spot off the side of the L_1 point. The inclination of ~ 78.4 degrees was not steep enough to allow total eclipses. Its photometric spectral type indicates a surface temperature of 5500 ± 200 K for the

Table 12. Sample of first ten TX CMi B, V, R_c, I_c observations.

ΔB	*HJD 2458800+*	ΔV	*HJD 2458800+*	ΔR	*HJD 2458800+*	ΔI	*HJD 2458800+*
–1.063	68.574	–1.100	68.577	–1.120	68.571	–1.064	68.572
–1.091	68.581	–1.101	68.584	–1.108	68.578	–1.073	68.579
–1.094	68.591	–1.094	68.594	–1.104	68.588	–1.082	68.589
–1.068	68.598	–1.080	68.601	–1.103	68.595	–1.099	68.596
–1.045	68.608	–1.050	68.610	–1.077	68.605	–1.072	68.606
–1.034	68.615	–1.040	68.618	–1.062	68.612	–1.090	68.613
–0.992	68.625	–0.993	68.628	–1.047	68.622	–1.013	68.623
–0.950	68.635	–0.927	68.637	–0.976	68.632	–0.969	68.632
–0.836	68.644	–0.819	68.647	–0.914	68.641	–0.894	68.642
–0.754	68.651	–0.736	68.654	–0.839	68.648	–0.815	68.649

Note: First ten data points of TX CMi B, V, R_c, I_c observations.
The full table is available through the AAVSO ftp site at ftp://ftp.aavso.org/public/datasets/samec492-txcmi.txt
(if necessary, copy and paste link into the address bar of a web browser).

Table 13. Sample of first ten DW CMi B, V, R_c, I_c observations.

ΔB	*HJD 2458800+*	ΔV	*HJD 2458800+*	ΔR	*HJD 2458800+*	ΔI	*HJD 2458800+*
0.078	68.574	0.008	68.577	–0.046	68.571	–0.027	68.572
0.035	68.581	–0.026	68.584	–0.043	68.578	–0.035	68.579
0.022	68.591	–0.018	68.594	–0.068	68.588	–0.071	68.589
0.041	68.598	–0.027	68.601	–0.071	68.595	–0.097	68.596
0.043	68.608	0.018	68.618	–0.067	68.605	–0.093	68.606
0.061	68.615	0.079	68.628	–0.040	68.612	–0.082	68.613
0.129	68.625	0.114	68.637	–0.017	68.622	–0.014	68.623
0.158	68.635	0.237	68.647	0.043	68.632	0.022	68.632
0.266	68.644	0.338	68.654	0.108	68.641	0.091	68.642
0.378	68.651	0.547	68.663	0.186	68.648	0.200	68.649

Note: First ten data points of TX CMi B, V, R_c, I_c observations.
The full table is available through the AAVSO ftp site at ftp://ftp.aavso.org/public/datasets/samec492-dwcmi.txt
(if necessary, copy and paste link into the address bar of a web browser).

primary component, making it a solar-type binary. Such a main sequence star would have a mass of $\sim 0.94\,M_\odot$ and the secondary (from the mass ratio) would have a mass of $\sim 1.03\,M_\odot$ making the secondary star over massive for its type and very similar to the primary component.

The period and epoch were used as iterating parameters for both of the solutions. One can see from the solution plots (Figures 17, 18, 21, and 22) that the data (phased with the linear ephemerides) fits th Wilson-Devinney phased solution plots very well.

11. Conclusions

The period is increasing for TX CMi with the mass ratio departing from unity so that the mass ratio becomes more extreme. We expect that this solar-type binary is undergoing magnetic braking and the binary will ultimately coalesce into a fast rotating late A-type single star. A spectroscopic radial velocity curve is needed to determine the actual mass ratio of the binary, but it is fairly assured that it is between $m_1/m_2 = 0.8$ and 1.2.

The period of DW CMi is decreasing. The occurrence of a spot and the period change does lend us to believe that the star is undergoing magnetic braking so we expect the future scenario to be much like that stated for TX CMi. The mass ratio is less determinable, however, and could range as much as 0.55 to 1.40. If q is >1.0, as the q-search gives, the system is a W-type W UMa binary (more massive star is the cooler one.) Radial velocity curves are very much needed to obtain the actual mass ratio and absolute (not relative) system parameters. Tables 8 and 12 give estimated parameters. Observations for DW CMi and TX CMi are given in Tables 13 and 14.

12. Acknowledgement

I wish to think the physics students from Appalachian State University that have helped with the observations.

References

Bradstreet, D. H., and Steelman, D. P. 2002, *Bull. Amer. Astron. Soc.*, **34**, 1224.

Brát, L., Zejda, L. M., and Svoboda, P. 2007, *B.R.N.O. Contrib.*, No. 34, 1.

Caton, D., Samec, R., and Faulkner, D. 2021, *Bull. Amer. Astron. Soc.*, **53**, e-id 2021n1i339p24.

Dvorak, S. W. 2005, *Inf. Bull. Var. Stars*, No. 5603, 1.

Gessner, H. 1966, *Veröff. Sternw. Sonneberg*, **7**, 61.

Hoffmeister, C. 1929, *Mitt. Sternw. Sonneberg*, **16**, 1.
Hubscher, J. 2007, *Inf. Bull. Var. Stars*, No. 5802, 1.
Hubscher, J. 2015, *Inf. Bull. Var. Stars*, No. 6152, 1.
Hubscher, J., and Lehmann, P. B. 2015, *Inf. Bull. Var. Stars*, No. 6149, 1.
Hubscher, J., Lehmann, P. B., and Walter, F. 2012, *Inf. Bull. Var. Stars*, No. 6010, 1.
Hubscher, J., Paschke, A., and Walter, F. 2006, *Inf. Bull. Var. Stars*, No. 5731, 1.
Hubscher, J., and Walter, F. 2007, *Inf. Bull. Var. Stars*, No. 5761, 1.
Kochanek, C. S., *et al.*, G. 2017, *Publ. Astron. Soc. Pacific*, 129, 104502.
Krajci, T. 2006, *Inf. Bull. Var. Stars*, No. 5690, 1.
Paschke, A. 1990, *BBSAG Bull.*, No. 95, 6.
Paschke, A. 1992, *BBSAG Bull.*, No. 102, 9.
Paschke, A. 1994, *BBSAG Bull.*, No. 106, 7.
Paschke, A. 2003, in Diethelm, R., *Inf. Bull. Var. Stars*, No. 5438, 3.
Paschke, A. 2012, *Open Eur. J. Var. Stars*, **147**, 1.
Pojmański, G. 2002, *Acta. Astron.*, **52**, 397.
Polster, J., Zejda, M., and Safar, J. 2005, *Inf. Bull. Var. Stars*, No. 5700, 10.
Polster, J., Zejda, M., and Safar, J. 2006, *Inf. Bull. Var. Stars*, No. 5700, 4.
Samec, R., Caton, D., Ray, J., Waddell, R., and Gentry, D. 2021, *Bull. Amer. Astron. Soc.*, 53, e-id 2021n1i128p01.
Samolyk, G. 2010, J. *Amer. Assoc. Var. Star Obs.*, **38**, 85.
Samus N. N., Kazarovets E. V., Durlevich O. V., Kireeva N. N., and Pastukhova E. N. 2017, *Astron. Rep.*, **61**, 80 (*General Catalogue of Variable Stars: Version GCVS 5.1*, http://www.sai.msu.su/groups/cluster/gcvs/gcvs).
Shappee, B. J., *et al.* 2014, *Astrophys. J.*, **788**, 48.
van Hamme, W. V., and Wilson, R. E. 1998, *Bull. Amer. Astron. Soc.*, **30**, 1402.
Wilson, R. E. 1990, *Astrophys. J.*, **356**, 613.
Wilson, R. E. 1994, *Publ. Astron. Soc. Pacific*, **106**, 921.
Wilson, R. E., and Devinney, E. J. 1971, *Astrophys. J.*, **166**, 605.
Zacharias, N., *et al.* 2010, *Astron. J.*, **139**, 2184.
Zejda, M. 2004, *Inf. Bull. Var. Stars*, No. 5583, 1.
Zejda, M., Mikulasek, Z., and Wolf, M. 2006, *Inf. Bull. Var. Stars*, No. 5741, 1.